Molecular characterization of ER Stress sensor IRE1α and IRE1β and their expression analysis in response to different fatty acid in grass carp (Ctenopharyngodon idellus)

Zhiguang Chang
Northwest Agriculture and Forestry University
Minghui Yang
Northwest Agriculture and Forestry University
Hong Ji (jihong0405@hotmail.com)
Northwest A&F University https://orcid.org/0000-0002-6383-776X

Research Article

Keywords: IRE1, fatty acids, autophagy, inflammation, Ctenopharyngodon idellus

Posted Date: March 8th, 2021

DOI: https://doi.org/10.21203/rs.3.rs-167447/v1

Molecular characterization of ER Stress sensor IRE1α and IRE1β and their expression analysis in response to different fatty acid in grass carp (*Ctenopharyngodon idellus*)

Zhiguang Chang[1], Minghui Yang[1], Hong Ji[1]*

[1] College of Animal Science and Technology, Northwest A&F University, Yangling, Shaanxi Province, 712100, China.

*Corresponding author: College of Animal Science and Technology, Northwest A&F University, Yangling, Shaanxi Province, 712100, China.

Tel/Fax: +86-29- 87092585

E-mail: jihong@nwsuaf.edu.cn

Abstract: Inositol-requiring enzyme 1 (IRE1) is the most evolutionarily conserved endoplasmic reticulum (ER) membrane protein. Here, we identified and analyzed two IRE isoforms (IRE1α and IRE1β) in grass carp (*Ctenopharyngodon idellus*). The coding sequences of IRE1α and IRE1β were 3096 and 2835 nucleotides, and they encoded proteins of 1031 and 944 amino acids, respectively. Each of the two IRE1s proteins had four PPQ domains, a transmembrane helix region, an S_TKc and a PUG domain, which were relatively conserved in comparison to mammals. qRT-PCR revealed that IRE1α was the highest in liver and brain, whereas the highest expression of IRE1β expressed was found in the hindgut, which may be closely related with their role. Moreover, we have compared the effect of saturated (palmitic acid, PA) , monounsaturated fatty acid (oleic acid, OA) and polyunsaturated fatty acids (Docosahexaenoic acid, DHA) on ER stress in CIK cells, and found that PA and DHA induced UPR-related gene expression in dose-dependent, and OA increased expression of IRE1α and decreased expression of IRE1β, ATF4 and ATF6 at lower doses. Additionally, our studies revealed that blocking IRE1α pathway using specific inhibitor 4μ8c, subsequently reversed PA-induced autophagy and inflammation, indicating the role of IRE1α in mediating PA-induced CIK cells. Taken together, the study demonstrated the IRE1α and IRE1β that likely have an important role in physiological processes induced by fatty acids in grass carp.

Keywords: IRE1, fatty acids, autophagy, inflammation, *Ctenopharyngodon idellus*

1. Introduction

The endoplasmic reticulum (ER) is a dynamic intracellular organelle and plays vital roles in cellular homeostasis, development, and stress responsiveness (Bravo et al., 2013). Any physiological or pathological perturbation can disrupt ER homeostasis and resulting in ER stress (Kaufman, 1999), such as lipid accumulation, reactive oxidative stress (ROS), protein overload, iron imbalance, hypoxia and viral infections (Ron and Walter, 2007). To combat the deleterious effects of ER stress, cells activate the unfolded protein response (UPR). The UPR includes three major simultaneous response pathways, namely inositol requiring enzyme 1 (IRE1), protein kinase RNA-like ER kinase (PERK), and activating transcription factor 6(ATF6) (Kaufman, 2002; Ron and Walter, 2007). Upon ER stress, activation of these three sensors can trigger pro-inflammatory response or cell apoptosis that is critically involved in the pathogenesis of a variety of diseases, such as obesity, type 2 diabetes, and age-associated pathogenesis (Bhattarai et al., 2020; Hummasti and Hotamisligil, 2010).

Inositol-requiring enzyme 1 (IRE1) was originally identified as a primary transducer of Unfolded Protein Response (UPR) (Tirasophon et al., 1998). IRE1 is the most evolutionarily conserved sensor and is found from yeast to metazoans (Acosta-Alvear et al., 2018). On ER stress, IRE1 is activated through trans-autophosphorylation and dimerization/oligomerization (Hetz, 2012), and then splices the mRNA encoding X-box binding protein 1 (XBP1) via its RNase activity to generate XBP1s (Shemorry et al., 2019). In turn, XBP1s activates transcriptional programs that regulate a subset of UPR- and non-UPR-associated genes (Wang et al., 2017). Moreover, IRE1α can recruit TRAF2, leading to activation of c-Jun N-terminal kinase (JNK)-mediated signaling pathway associated with inflammatory and metabolic diseases (Urano et al., 2000). Together, these findings reveal the IRE1α-XBP1 signaling pathway was involved in regulation of cellular processes including ER-associated degradation, inflammatory signaling, cell proliferation and membrane biogenesis (Stewart et al., 2017).

In farmed fish, HFD commonly cause excess fat accumulation, which leading to liver injury and lipid metabolism disorders (Cao et al., 2019). Therefore, focused on the mechanism of lipid metabolism by excessive fatty acid in different tissues of fish would be highly beneficial. In this study, we cloned and identified the IRE1α and IRE1β homologs named IRE1α and IRE1β from *Ctenopharyngodon idellus*, and detected their expression patterns in response to different fatty acid or thapsigargin (TG) induced ER stress in CIK cells. We also investigated whether inhibition of IRE1α markedly restored PA-induced autophagy and inflammation-related genes. These preliminary findings help to understand the role of IRE1 in grass carp.

2. Materials and methods

2.1 Cloning of IRE-1 cDNA

Total RNA was extracted from various tissues of healthy grass carp by using Trizol reagent (Invitrogen). First strand cDNA synthesis was carried out using a PrimeScript 1st Strand cDNA Synthesis Kit (TaKaRa) according to the manufacturer's instructions. PCR amplification primers were designed based on the IRE-1 gene from the grass carp transcriptome database (Table 1). The PCR products were gel-extracted and ligated into pMD18-T (Takara). Following transformation into competent Escherichia coli DH5α cells, positive clones were screened using ampicillin selection and colony PCR and then sequenced (Sangon Biotech).

2.2 Sequence and Phylogenetic analysis

The amino acid sequence was predicted using the translate tool, and the molecular weight, isoelectric point (*p*I), and net charge of the peptides were calculated using the ProtParam tool, both available on the ExPASy molecular biology server (http://www.expasy.org/tools). The protein domain features were predicted by SMART (http://smart.embl-heidelberg.de/). Multiple sequence alignments were generated using Clustal W (version 1.83). The phylogenetic tree was constructed using the Neighbor-Joining method in MEGA 7.0 software with 1000 bootstrap replicates.

2.3 Cells culture

Ctenopharyngodon idellus kidney (CIK) cells line was obtained from China Center for Type Culture Collection (CCTCC, Wuhan) and maintained in DMEM medium supplemented with 10% fetal bovine serum (Gibco, USA), and in a humid atmosphere of 5% CO_2 at 28°C.

2.4 Fatty acid treatment

Palmitic acid (PA), Docosahexaenoic acid (DHA) and oleic acid (OA) were purchased from Sigma-Aldrich, and a stock solution was prepared by dissolving 100% ethanol at 50 mM and stored at −80 °C. Cells were treated with the indicated concentrations of fatty acid (50-200 μM) dissolved in media containing 1% fatty acid-free BSA for 24 hours.

2.5 Quantitative real-time PCR (qRT-PCR) analysis

Total RNA was extracted from tissue and cell samples, and then reverse transcribed to obtain cDNA. The obtained cDNA were served as template for real-time quantitative PCR (qPCR) analysis to examine the expression level of six RBR genes. Three replicates were conducted for each sample and β-actin as an internal reference gene. Amplification reactions were performed in triplicate in 20 μl containing 1.0 μl cDNA sample, 10 μl 2×SYBR premix Ex Taq (TaKaRa), 0.4 μl of each primer, and 8.2 μl ddH2O. The program was performed as follows: 1cycle of 94 °C/5 min; 40 cycles of 94 °C/30 s, 60°C/30 s, and 72 °C/30 s. The obtained data were evaluated using the $2^{-\Delta\Delta Ct}$ method and then statistically analyzed. The primers for Q-PCR were listed in Table 1.

2.6 Statistical analyses

Each experiment was done independently at least three times with similar results. Results were expressed as mean ± S.D. All data were expressed as Mean _SEM (N=3) and the groups denoted by stars (*) represent a significant difference at $P < 0.05$ from controls (** means $P < 0.01$).

3. Results

3.1 Sequence analysis of IRE1α and IRE1β cDNA

The full-length of IRE1α cDNAwas 4038 bp (GenBank accession no. MH370854), and the ORF was 3096 bp encoding 1031 amino acids (Supplement Fig.1). The predicted molecular weight and isoelectric point of the deduced IRE1α protein was 116.3 kDa and 6.13, respectively. The full-length of IRE1β cDNA was 3504 bp (GenBank accession no. MK616212), and the ORF was 2835 bp encoding 944 amino acids (Supplement Fig.2). The predicted molecular weight and isoelectric point of the deduced IRE1β protein was 105.2 kDa and 6.24, respectively. The predicted IRE1α and IRE1β protein shared the conservative signal peptide domain, pyrrolo-quinoline quinine domains (PPQ), Ser/Thr protein kinase domain (S_TKc) and peptide N-glycanase domain (PUG) (Supplement Fig.3). Moreover, the predicted IRE1α and IRE1β protein consist of conserved domains that are critical for their function, that contains the putative signal peptide, ER-luminal domain, transmembrane region, and kinase and RNase subdomains, which displays a very high homology to human IRE1α and IRE1β, respectively (Fig.1).

3.2 Phylogenetic analysis based on IRE1α and IRE1β amino acid sequence

To determine the evolutionary status of IRE1α and IRE1β, a phylogenetic tree was constructed based on the amino acid sequence of IRE1α and IRE1β, respectively (Fig.2). According to the tree, mammals and fish can be separated into two branches. Moreover, multiple sequence alignment and amino acid identity comparisons indicated that IRE1α and IRE1β share a sequence identity with other species, exhibiting 48.16–92.43 % and 51.65–92.90 % AA sequence identities, respectively (Supplement Fig.4 and Supplement Fig.5). Moreover, the encoded IRE1α protein, consisting of 1031 amino acids, displays a very high homology to human IRE1α (73.46%). The encoded IRE1β protein, consisting of 944 amino acids, displays a very high homology to human IRE1β (52.69%).While, the amino acid sequence of IRE1α and IRE1β has 48% identity.

3.3 Expression of IRE1α and IRE1β mRNA in different tissues

Expression levels of the IRE1α and IRE1β transcript in twelve tissues of grass carp were analyzed to determine its tissue distribution. The IRE1α mRNA levels was the highest in liver and brain, followed by mid-intestine, kidney, heart, hindgut, gill, spleen, head kidney and lowest in red muscle and white muscle, whereas the highest expression of IRE1β expressed was found in the hindgut, with a moderate level of expression observed in the heart, mid-intestine, foregut, gill,

white muscle, brain, liver, but only weak expression in the spleen, head kidney, kidney and red muscle (Fig.3). indicate that may play different roles in different tissues in grass carp.

3.4 Expression patterns of IRE1α and IRE1β in response to ER stress in CIK cells

In order to determine the expression pattern of IRE1α and IRE1β mRNA in response to ER stress, we treated CIK cells with an ER stress inducer, such as tunicamycin (TM) or thapsigargin (TG). First, Figure 2B shows that TM and TG treatment could activate the expression of ER stress-related genes, such as GRP78, ATF6 and CHOP. Moreover, the expression of IRE1α and IRE1β were also up-regulated in a dose-dependent manner by TG treatment, but IRE1β expression was higher than IRE1α expression in all treatments. In addition, we also found that the levels of TNFα and NF-κB were all increased after TG stimulation, suggesting that ER-stress related inflammation was activated (Fig.4). These results suggest that IRE1α and IRE1β have different expression pattern in response to ER stress and involve in ER-stress induced inflammatory reactions in CIK cells.

3.5 Expression patterns of IRE1α and IRE1β in response to different fatty acids

To compare the effects of different fatty acids on IRE1, we incubated CIK cells for 24 h with OA, PA, or DHA at concentrations ranging from 50 to 200μM. The results revealed that different concentrations of DHA and PA could significantly increase the mRNA levels of ER stress-related genes, such as GRP78, ATF6 and CHOP. Whereas OA could decrease the expression of ER related genes, such as GRP78, CHOP and ATF6, except IRE1α (Fig.5). Moreover, DHA and OA treatment showed a significant increase in the number of lipid droplets, compared with PA (data not shown). These results suggest that IRE1α and IRE1β have different expression profile in response to different fatty acids induced metabolism of lipid droplets in CIK cells.

3.6 Inhibition of IRE1α ameliorates PA induced autophagy and inflammation

IRE1α is a multi-functional protein (Riaz et al., 2020), we wanted to examine the importance of IRE1α in PA induced CIK cell inflammation and autophagy, CIK cells were exposed to PA, with or without 4μ8c. As shown in Fig.6, IRE1α inhibition significantly inhibited the ATG5, ATG7 and Beclin-1 expression induced by PA. Moreover, 4μ8c successfully reduced the levels of inflammation -related gene expression induced by PA. These results indicated that IRE1α is involved in PA-induced autophagy and inflammation in CIK cells.

4. Discussion

IRE1 exists in two isoforms: IRE1α/ERN1 and IRE1β/ERN2.To date, the function of IRE1α was identified from *Larimichthys crocea* (Zhang et al., 2020). In this study, we cloned the grass carp IRE1α and IRE1β cDNA. Phylogenetic tree analysis showed that IRE1 protein of grass carp were closely related to that of *Sinocyclocheilus anshuiensi* . Similar to mammalian IRE1, the IRE1

protein of grass carp also has conserved domain, including an endoribonuclease (RNase) and a serine/threonine kinase (Fig.1). These results confirmed that IRE1 is highly conserved among different species. Consistent with previous study (Bertolotti et al., 2001; Martino et al., 2013), our results show that IRE1α was expressed in all tissues examined, with the highest expression level in liver, and IRE1β was highly expressed in the intestine in grass carp. Some studies indicated that IRE1β plays a constitutive role in lipid metabolism through MTP mRNA degradation in intestinal epithelial (Iqbal et al., 2008; Tsuru et al., 2013). Recent studies suggest that IRE1β and IRE1α appear to have distinct enzymatic activities, and IRE1β acts as a negative regulator of IRE1α in intestinal epithelial cells (Grey et al., 2020), but the exact regulatory function remain unknown. Obviously, they have different physiological functions.

IRE1 can be activated lipid-dependent in yeast and mammalian (Robblee et al., 2016; Volmer and Ron, 2015). Previous studies also demonstrated that DHA was incorporated into TAG as well as OA, PA was not incorporated into TAG (Caviglia et al., 2011). In this study, we compared the effects of OA, PA and DHA regarding their ability to induce ER stress and lipogenesis. Our results found that OA and DHA can significantly induce the formation of TAG, but they did not significantly induce ER stress. In contrast, PA can induce endoplasmic reticulum stress more effectively, but no obvious lipid droplets were observed in CIK cells. These findings suggest that TAG itself does not appear to be the mediator of fatty acid-induced ER stress (Caviglia et al., 2011), although the exact mechanism remains unclear. Moreover, it has been show that human IRE1α activation by membrane lipid saturation (Cho et al., 2019). Here, we found that compared to DHA and OA, PA induced IRE1α and IRE1β expression more rapidly and dramatically, and the expression of IRE1β is higher than that of IRE1α, implying that IRE1β rather than IRE1α was closely related with lipid saturation in grass carp.

Multiple mechanisms are involved in PA-induced kidney injury in human, including ER stress, autophagy and inflammation (Park et al., 2019). Previous reports have also demonstrated that IRE1α has emerged as a key regulator of autophagy and inflammation (Bao et al., 2018; Cheng et al., 2014; Junjappa et al., 2018). Here, we found that inhibition of IRE1α attenuates PA-induced inflammation and autophagy. How IRE1β affects these interactions and regulatory mechanisms also remain to be determined. Interestingly, treatment of CIK cells with 4μ8C, which are IRE1α-specific inhibitors, reduced the IRE1β expression, these may be due to they complement each other's role in protein folding homeostasis (Tschurtschenthaler et al., 2017). Taken together, our results demonstrated that IRE1α inhibition protected from PA-induced autophagy and inflammation in CIK cells.

In conclusion, we cloned the full-length sequences of IRE1α and IRE1β, and confirmed

IRE1α signaling is activated in response to different fatty acids in CIK cells. Importantly, we found that IRE1α integrates autophagy and inflammation. However, the mechanisms of IRE1β remain to be further explored in grass carp.

Availability of data and material

Data and materials are available upon request.

Competing interests

The authors disclose no conflicts of interest. All the authors listed have approved to submit to your journal.

Funding

This study was supported by the National Nature Science Foundation of China (Grant Number: 31772863).

Authors' contributions

Zhiguang Chang performed the experiments and wrote the manuscript; Minghui Yang collected the literature; Hong Ji primarily revised the manuscript. All authors have read and approved the final manuscript.

Ethics declarations

All procedures were performed in accordance with the Guide for Care and Use of Laboratory Animals and approved by the Northwest A&F University Institutional Animal Care and Use Com mittee.

References

Acosta-Alvear, D., Karagoz, G.E., Frohlich, F., Li, H., Walther, T.C., Walter, P., 2018. The unfolded protein response and endoplasmic reticulum protein targeting machineries converge on the stress sensor IRE1. eLife 7.

Bao, Y., Pu, Y., Yu, X., Gregory, B.D., Srivastava, R., Howell, S.H., Bassham, D.C., 2018. IRE1B degrades RNAs encoding proteins that interfere with the induction of autophagy by ER stress in Arabidopsis thaliana. Autophagy 14, 1562-1573.

Bertolotti, A., Wang, X., Novoa, I., Jungreis, R., Schlessinger, K., Cho, J.H., West, A.B., Ron, D., 2001. Increased sensitivity to dextran sodium sulfate colitis in IRE1beta-deficient mice. The Journal of clinical investigation 107, 585-593.

Bhattarai, K.R., Chaudhary, M., Kim, H.R., Chae, H.J., 2020. Endoplasmic Reticulum (ER) Stress Response Failure in Diseases. Trends in cell biology.

Bravo, R., Parra, V., Gatica, D., Rodriguez, A.E., Torrealba, N., Paredes, F., Wang, Z.V., Zorzano, A., Hill, J.A., Jaimovich, E., Quest, A.F., Lavandero, S., 2013. Endoplasmic reticulum and the unfolded protein response: dynamics and metabolic integration. International review of cell and molecular biology 301, 215-290.

Cao, X.F., Dai, Y.J., Liu, M.Y., Yuan, X.Y., Wang, C.C., Huang, Y.Y., Liu, W.B., Jiang, G.Z., 2019. High-fat diet induces aberrant hepatic lipid secretion in blunt snout bream by activating endoplasmic reticulum stress-associated IRE1/XBP1 pathway. Biochimica et biophysica acta. Molecular and cell biology of lipids 1864, 213-223.

Caviglia, J.M., Gayet, C., Ota, T., Hernandez-Ono, A., Conlon, D.M., Jiang, H., Fisher, E.A., Ginsberg, H.N., 2011. Different fatty acids inhibit apoB100 secretion by different pathways: unique roles for ER stress, ceramide, and autophagy. Journal of lipid research 52, 1636-1651.

Cheng, X., Liu, H., Jiang, C.C., Fang, L., Chen, C., Zhang, X.D., Jiang, Z.W., 2014. Connecting endoplasmic reticulum stress to autophagy through IRE1/JNK/beclin-1 in breast cancer cells. International journal of molecular medicine 34, 772-781.

Cho, H., Stanzione, F., Oak, A., Kim, G.H., Yerneni, S., Qi, L., Sum, A.K., Chan, C., 2019. Intrinsic Structural Features of the Human IRE1alpha Transmembrane Domain Sense Membrane Lipid Saturation. Cell reports 27, 307-320 e305.

Grey, M.J., Cloots, E., Simpson, M.S., LeDuc, N., Serebrenik, Y.V., De Luca, H., De Sutter, D., Luong, P., Thiagarajah, J.R., Paton, A.W., Paton, J.C., Seeliger, M.A., Eyckerman, S., Janssens, S., Lencer, W.I., 2020. IRE1beta negatively regulates IRE1alpha signaling in response to endoplasmic reticulum stress. The Journal of cell biology 219.

Hetz, C., 2012. The unfolded protein response: controlling cell fate decisions under ER stress and beyond. Nature reviews. Molecular cell biology 13, 89-102.

Hummasti, S., Hotamisligil, G.S., 2010. Endoplasmic reticulum stress and inflammation in obesity and diabetes. Circulation research 107, 579-591.

Iqbal, J., Dai, K., Seimon, T., Jungreis, R., Oyadomari, M., Kuriakose, G., Ron, D., Tabas, I., Hussain, M.M., 2008. IRE1beta inhibits chylomicron production by selectively degrading MTP mRNA. Cell metabolism 7, 445-455.

Junjappa, R.P., Patil, P., Bhattarai, K.R., Kim, H.R., Chae, H.J., 2018. IRE1alpha Implications in Endoplasmic Reticulum Stress-Mediated Development and Pathogenesis of Autoimmune Diseases. Frontiers in immunology 9, 1289.

Kaufman, R.J., 1999. Stress signaling from the lumen of the endoplasmic reticulum: coordination of gene transcriptional and translational controls. Genes & development 13, 1211-1233.

Kaufman, R.J., 2002. Orchestrating the unfolded protein response in health and disease. The Journal of clinical investigation 110, 1389-1398.

Martino, M.B., Jones, L., Brighton, B., Ehre, C., Abdulah, L., Davis, C.W., Ron, D., O'Neal, W.K., Ribeiro, C.M., 2013. The ER stress transducer IRE1beta is required for airway epithelial mucin production. Mucosal immunology 6, 639-654.

Park, S.J., Kim, Y., Chen, Y.M., 2019. Endoplasmic reticulum stress and monogenic kidney diseases in precision nephrology. Pediatric nephrology 34, 1493-1500.

Riaz, T.A., Junjappa, R.P., Handigund, M., Ferdous, J., Kim, H.R., Chae, H.J., 2020. Role of Endoplasmic Reticulum Stress Sensor IRE1alpha in Cellular Physiology, Calcium, ROS Signaling, and Metaflammation. Cells 9.

Robblee, M.M., Kim, C.C., Porter Abate, J., Valdearcos, M., Sandlund, K.L., Shenoy, M.K., Volmer, R., Iwawaki, T., Koliwad, S.K., 2016. Saturated Fatty Acids Engage an IRE1alpha-Dependent Pathway to Activate the NLRP3 Inflammasome in Myeloid Cells. Cell reports 14, 2611-2623.

Ron, D., Walter, P., 2007. Signal integration in the endoplasmic reticulum unfolded protein response. Nature reviews. Molecular cell biology 8, 519-529.

Shemorry, A., Harnoss, J.M., Guttman, O., Marsters, S.A., Komuves, L.G., Lawrence, D.A., Ashkenazi, A., 2019. Caspase-mediated cleavage of IRE1 controls apoptotic cell commitment during endoplasmic reticulum stress. eLife 8.

Stewart, C., Estrada, A., Kim, P., Wang, D., Wei, Y., Gentile, C., Pagliassotti, M., 2017. Regulation of IRE1alpha by the small molecule inhibitor 4mu8c in hepatoma cells. Endoplasmic reticulum stress in diseases 4, 1-10.

Tirasophon, W., Welihinda, A.A., Kaufman, R.J., 1998. A stress response pathway from the endoplasmic reticulum to the nucleus requires a novel bifunctional protein kinase/endoribonuclease (Ire1p) in mammalian cells. Genes & development 12, 1812-1824.

Tschurtschenthaler, M., Adolph, T.E., Ashcroft, J.W., Niederreiter, L., Bharti, R., Saveljeva, S., Bhattacharyya, J., Flak, M.B., Shih, D.Q., Fuhler, G.M., Parkes, M., Kohno, K., Iwawaki, T., Janneke van der Woude, C., Harding, H.P., Smith, A.M., Peppelenbosch, M.P., Targan, S.R., Ron, D., Rosenstiel, P., Blumberg, R.S., Kaser, A., 2017. Defective ATG16L1-mediated removal of IRE1alpha drives Crohn's disease-like ileitis. The Journal of experimental medicine 214, 401-422.

Tsuru, A., Fujimoto, N., Takahashi, S., Saito, M., Nakamura, D., Iwano, M., Iwawaki, T., Kadokura, H., Ron, D., Kohno, K., 2013. Negative feedback by IRE1beta optimizes mucin production in goblet cells. Proceedings of the National Academy of Sciences of the United States of America 110, 2864-2869.

Urano, F., Wang, X., Bertolotti, A., Zhang, Y., Chung, P., Harding, H.P., Ron, D., 2000. Coupling of stress in the ER to activation of JNK protein kinases by transmembrane protein kinase IRE1. Science 287, 664-666.

Volmer, R., Ron, D., 2015. Lipid-dependent regulation of the unfolded protein response. Current opinion in cell biology 33, 67-73.

Wang, N., Zhao, F., Lin, P., Zhang, G., Tang, K., Wang, A., Jin, Y., 2017. Knockdown of XBP1 by RNAi in Mouse Granulosa Cells Promotes Apoptosis, Inhibits Cell Cycle, and Decreases Estradiol Synthesis. International journal of molecular sciences 18.

Zhang, J., Liu, Q., Pang, Y., Xu, X., Cui, K., Zhang, Y., Mai, K., Ai, Q., 2020. Molecular cloning and the involvement of IRE1alpha-XBP1s signaling pathway in palmitic acid induced - Inflammation in primary hepatocytes from large yellow croaker (Larimichthys crocea). Fish & shellfish immunology 98, 112-121.

351 Table. 1. PCR primer and interference sequence information in this study.

Primer name	Forward (5'→3')	Reverse (5'→3')	Application
IRE1αF1	AGTTGATAAACGCATTGAAC	ACCAGTGGAGTGTTTCCCTA	Gene cloning of IRE1α
IRE1αF2	CACTGTATGTAGGGAAACAC	TCTCTTCTCTGGCTCCATGC	Gene cloning ofIRE1α
IRE1αF3	CAGATGTTAAGCATGGAGCC	CTGGCATTTACTAACAAAAG	Gene cloning of IRE1α
IRE1βF1	TATTTGTTATTTTATTATAGGA	GCACAAGGGAGGTAGAAGCA	Gene cloning of IRE1β
IRE1βF2	AGACAGACTCTCATCTGTATG	TTTGTATGCATGTGTACTGGC	Gene cloning ofIRE1β
IRE1βF3	CCCTGTACGACTGCCAGTACA	GGCTGGAGATTCACGTAATCT	Gene cloning of IRE1β
IRE1α	CCTGCATGGTAGACATCTTCTC	TTCTCTGGCTCCATGCTTAAC	Real time RT-PCR
IRE1β	GTGGCAGGGTTCTACTTATGG	GCTCTCCTTTGTGAACTGGTAG	Real time RT-PCR
GRP78	TTCAAGCCGGAGTTCTGTCC	GTTGTCAGAAGCGGTGGAGA	Real time RT-PCR
CHOP	GCGTGGTATGAAGACCTACAG	CGCTGACCATCGTTTCCA	Real time RT-PCR
ATF6	AGCTGGAGGATCTTGGGGAT	TGATCGAGGGCTACTCCACA	Real time RT-PCR
TNFα	GATTGGAGAGTGAACCAGGAC	CCTGGCTGTAGACGAAGTAAAT	Real time RT-PCR
NF-κB	GAACATTTAACCCACGCAAGAG	GGCCTTTCCTGCCATCTAATA	Real time RT-PCR
XBP-1s	GGTCTTCTGAGTCCGCAGCAG	AGACTCAGTGTCTGCAGGGCC	Real time RT-PCR
IL-10	ATGCCAACCTCCTGTTCTTC	CACTTCCACCTGCTCCATATC	Real time RT-PCR
TGFβ1	GTGACGCCAGCATTGTATCTA	GTCAGCGTTGCTGGAATTTATC	Real time RT-PCR
ATG5	GGAGGAGATGTGGTTTGAGTATG	GCCCAGAACTGGTCGAATTTA	Real time RT-PCR
Beclin-1	AGCTCGACACATCCTTCAAC	CTGCGACTCAAGTTCTCCATAG	Real time RT-PCR
ATG7	TTTGAAGACTGTCTGAGCGG	GCCATTGTCAACTCGGAAAAG	Real time RT-PCR
β-actin	CGTGACATCAAGGAGAAG	GAGTTGAAGGTGGTCTCAT	Real time RT-PCR

352

353

354

355

356

357

358

359

Fig.1 Amino acid sequence alignment of the IRE1α and IRE1β in grass carp with homologs from human, respectively.Identical residues are marked by asterisks underline. Signal peptide and domains are as indicated.

Fig.2 Phylogenetic tree based on the protein sequences of IRE1α and IRE1β from grass carp and other species using the neighbor-joining (NJ) method in MEGA 5.0. Branch support values represent a percentage of 1000 bootstrap replicates.

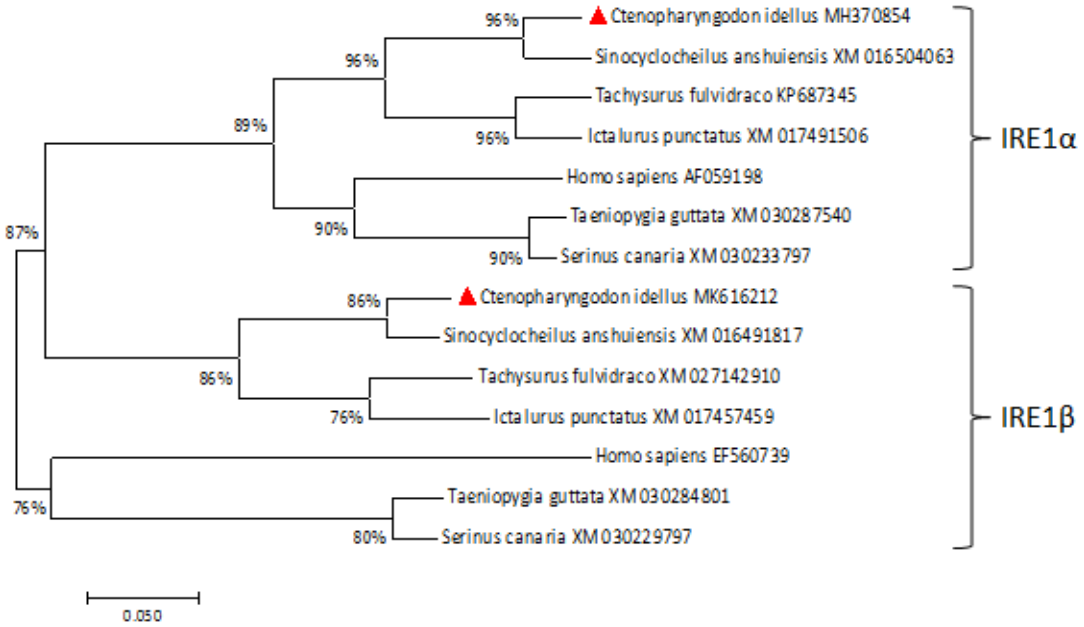

Fig.3 Expression profiles of IRE1α and IRE1β gene in 12 tissues of grass carp obtained by qPCR. The 12 tissues were heart (He), liver (Li), spleen (Sp), head kidney (Hk), kidney (Ki), brain (Br), foregut (Fg), mid-gut (Mg), hindgut (Hg), gill (Gi), red muscle (Rm) and white muscle (Wm). β-actin served as an internal control to calibrate the cDNA template for all of the samples.

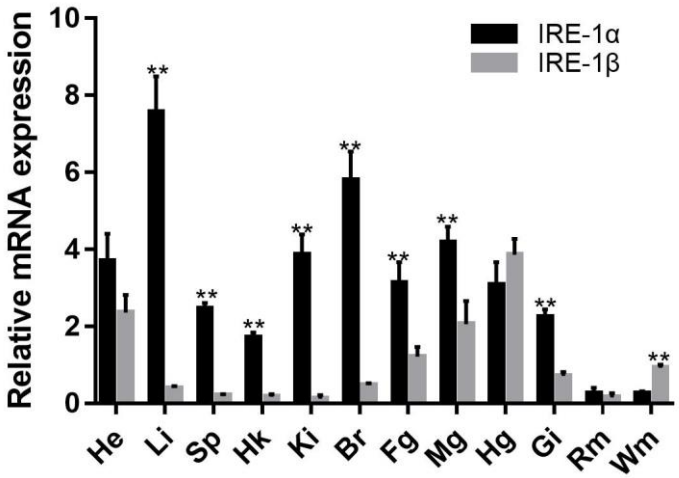

Fig.4 IRE1α and IRE1β levels were upregulated in response to ER stress in CIK cells. Cells were treated with TM (10μM) and TG (0, 2.5, 5, or 10μM) for 24 hours. The relative mRNA levels were detected by Real-time PCR.

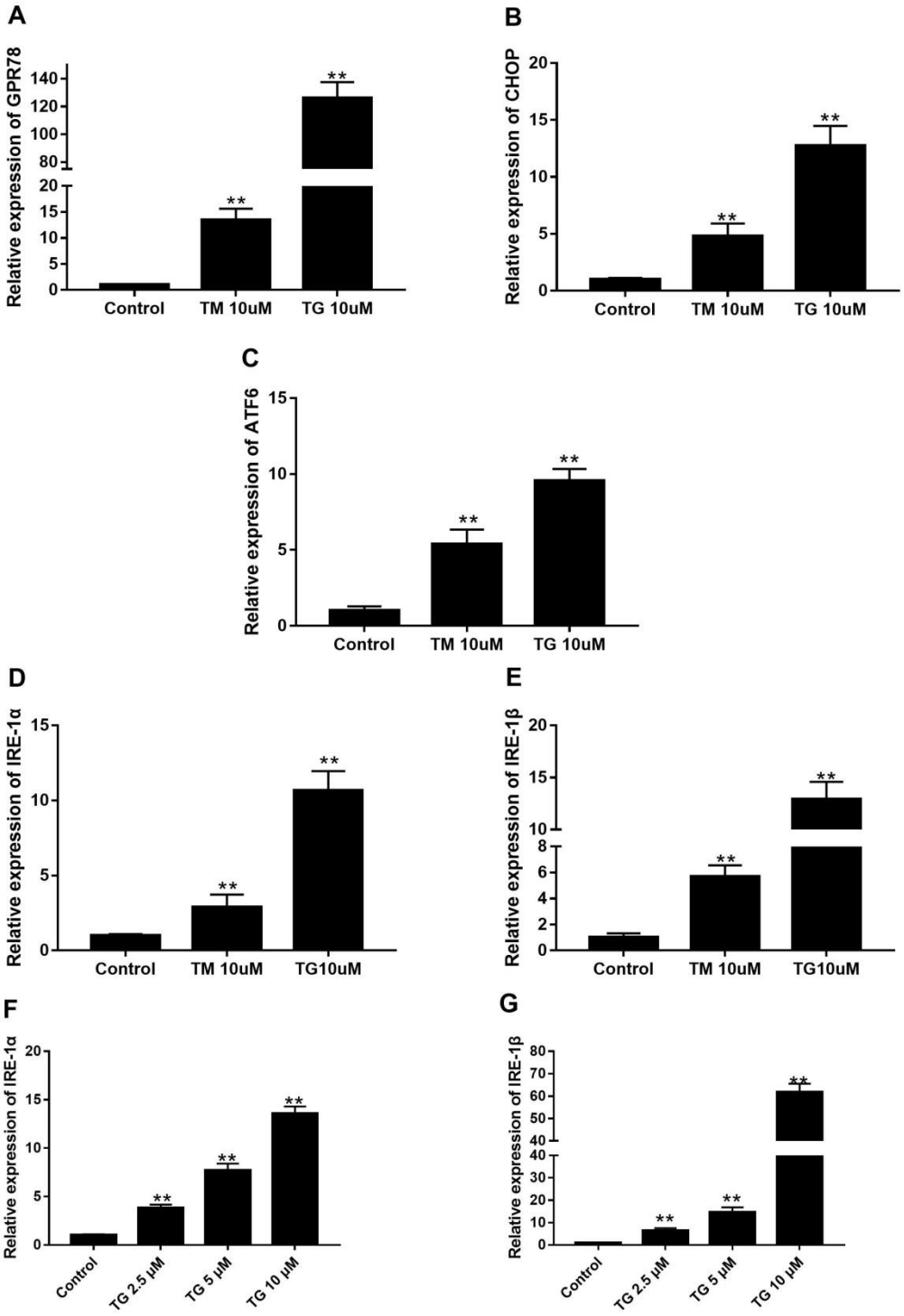

Fig.5 Effects of fatty acids on ER stress in CIK cells. CIK cells were incubated with various concentrations of fatty acids for 24 hours. Cells treated with BSA as the control, after incubation, Total RNA was extracted and then quantified using Real-time PCR.

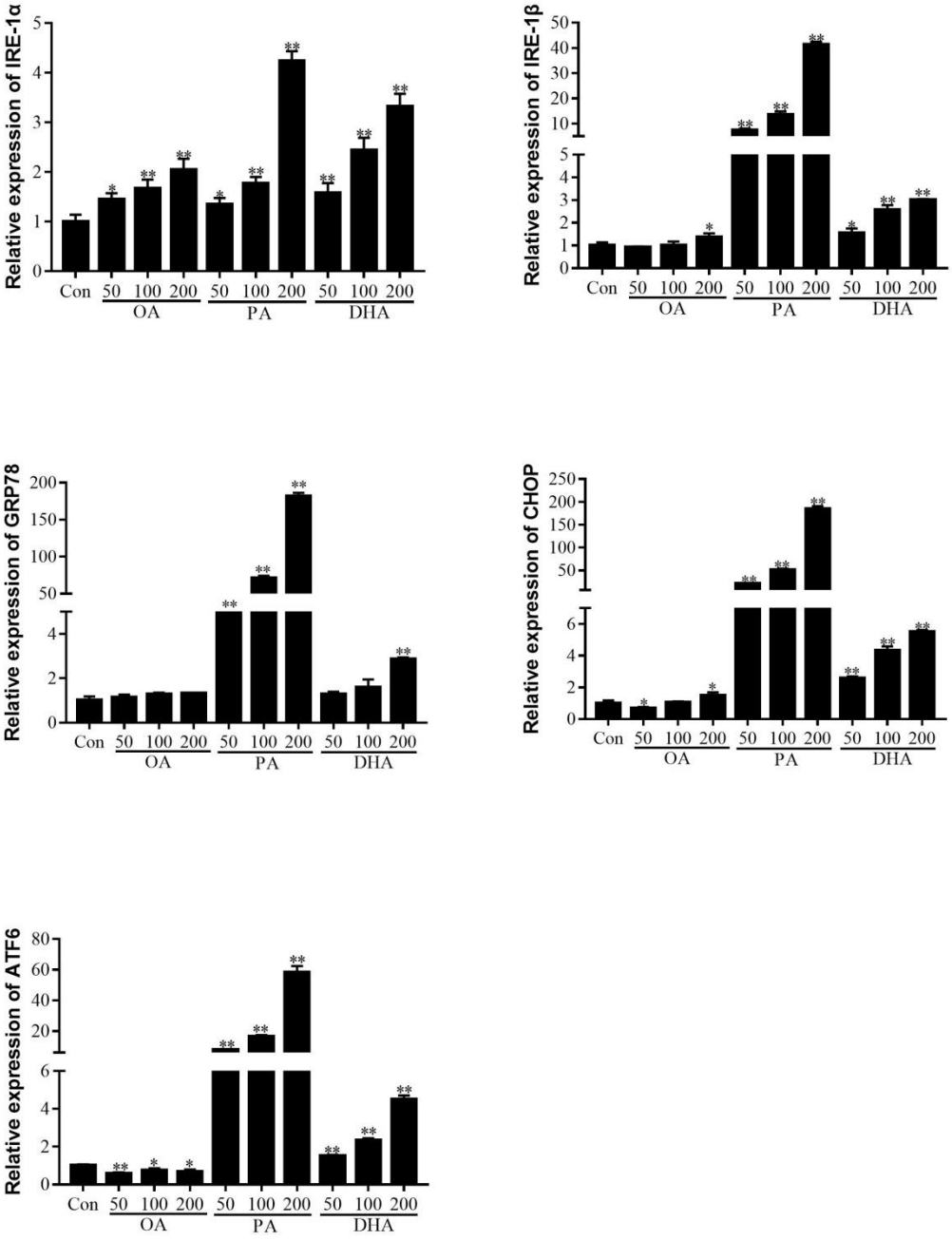

Fig.6 Inhibition of IRE1α ameliorates PA induced autophagy and inflammation. CIK cells were later either pretreated with 4μ8C for 4 h, followed by treatment with PA (200 μM) for 24 h. CIK cells treated with vehicle (DMSO) and BSA were used for control. Total RNA was extracted and then quantified using Real-time PCR. *significantly different compared with controls ($P < 0.05$); # significantly different compared with PA ($P < 0.05$).

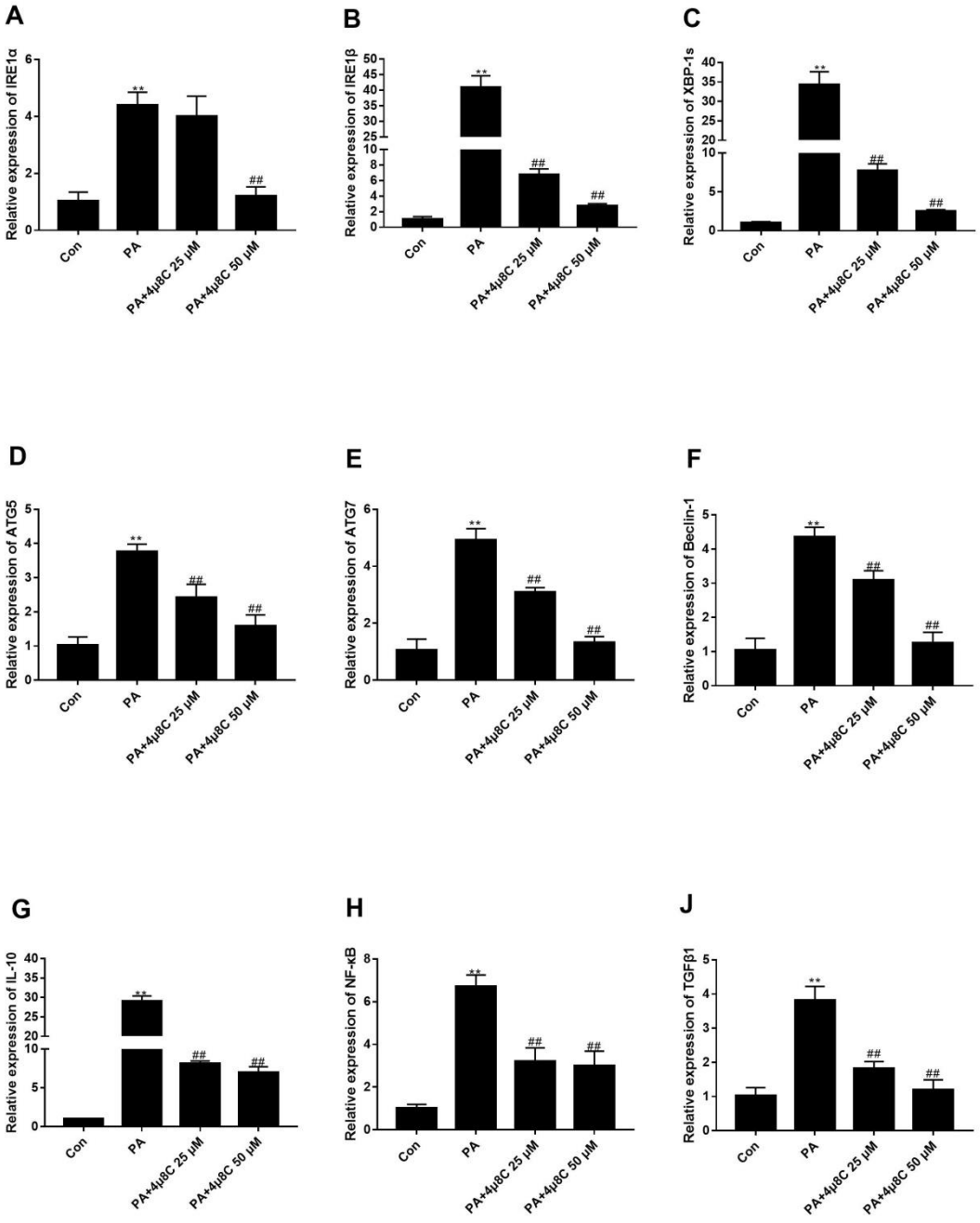

Figures

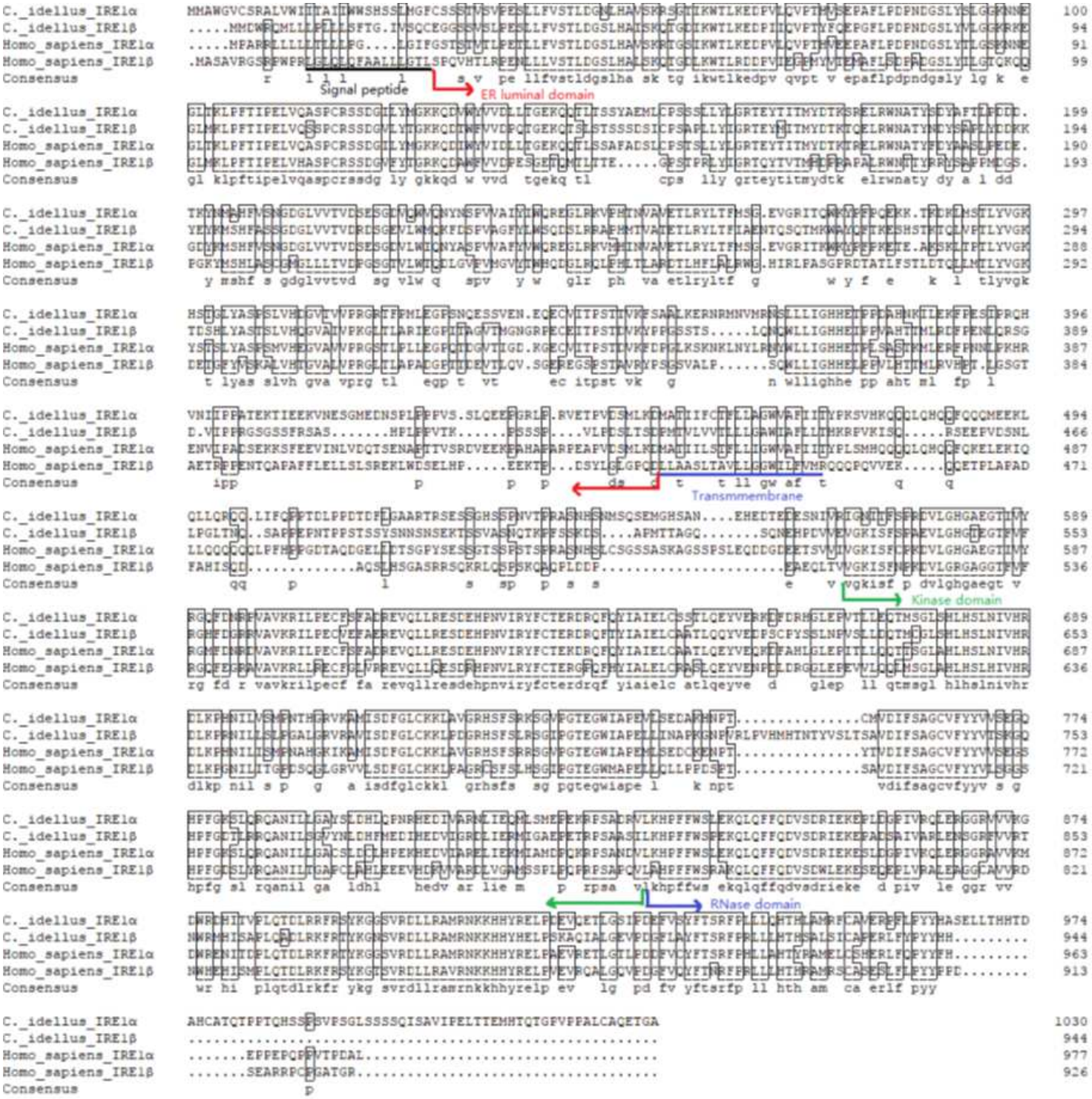

Figure 1

Amino acid sequence alignment of the IRE1α and IRE1β in grass carp with homologs from human, respectively.Identical residues are marked by asterisks underline. Signal peptide and domains are as indicated.

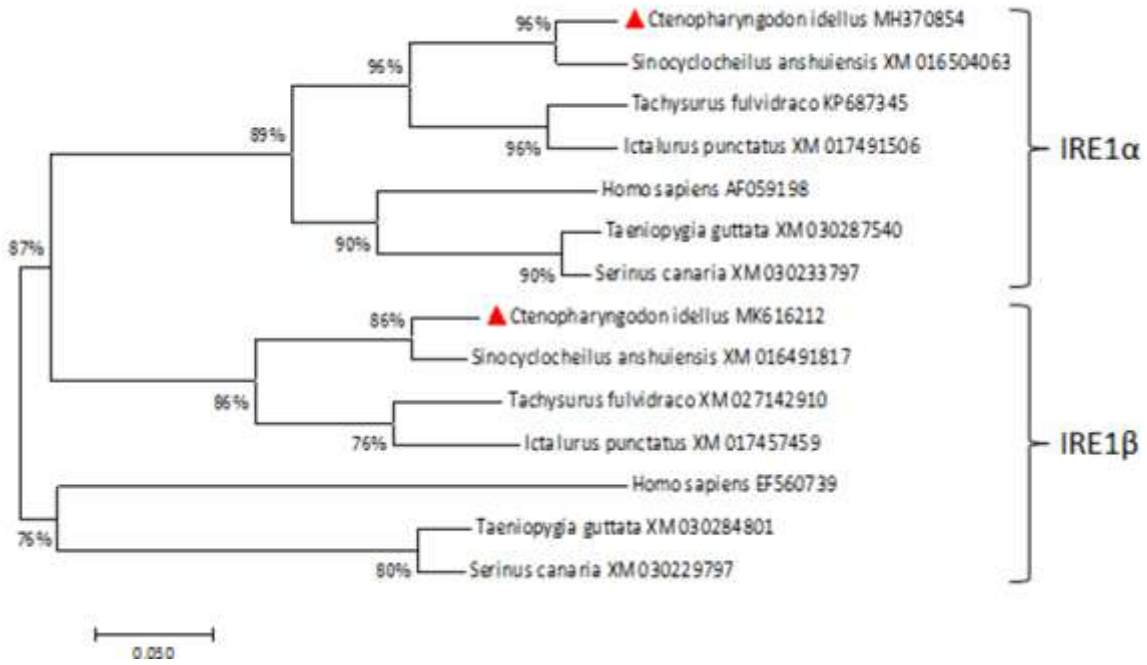

Figure 2

Phylogenetic tree based on the protein seq uences of IRE1α and IRE1β from grass carp and other species using the neighbor joining (NJ) method in MEGA 5.0 . Branch support values represent a percentage of 1000 bootstrap replicates.

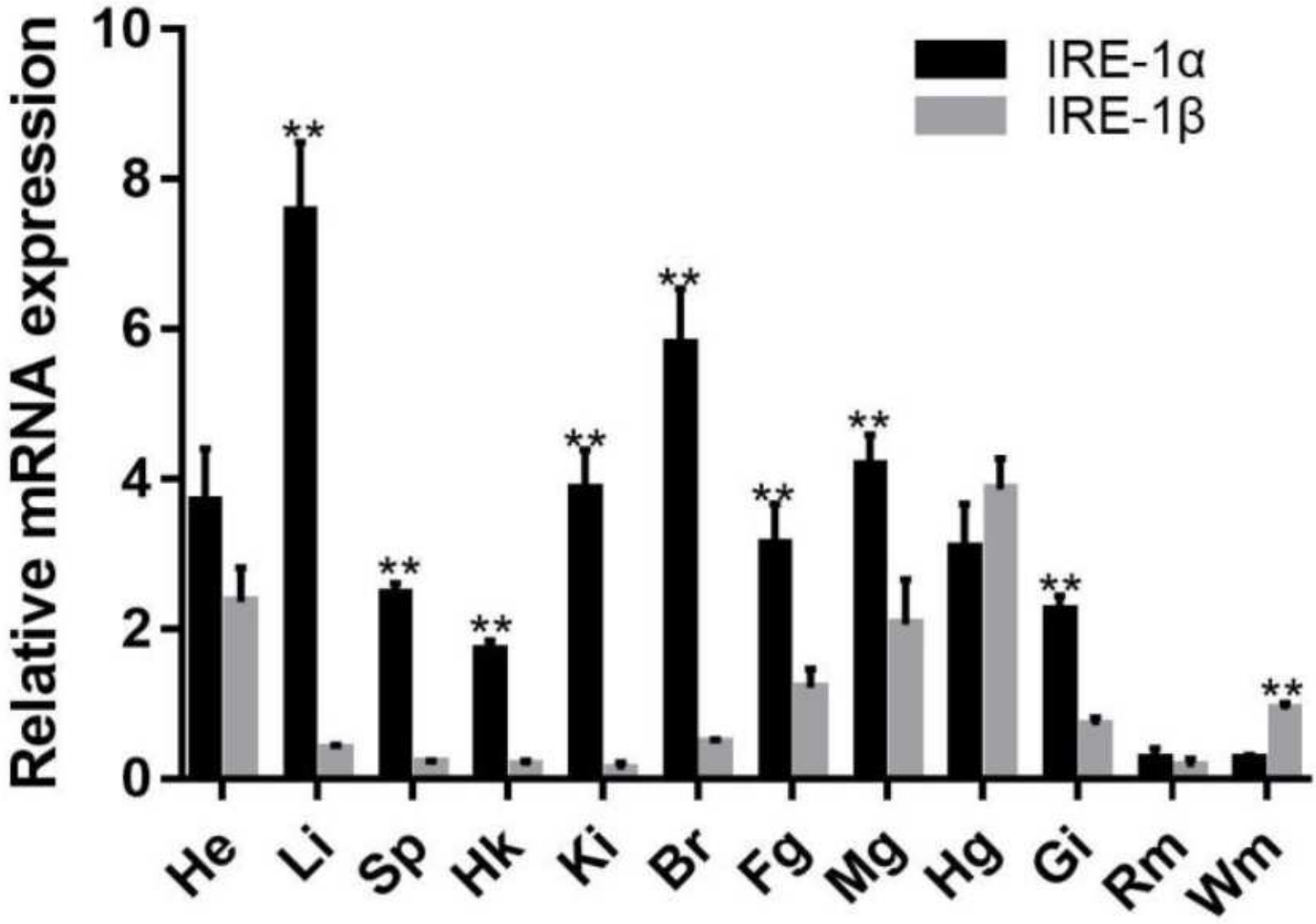

Figure 3

Expression profiles of IRE1α and IRE1β gene in 12 tissues of grass carp obtained by qPCR. The 12 tissues were heart (He), liver (Li), spleen (Sp), head kidney (Hk), kidney (Ki), brain (Br), foregut (Fg), mid gut (Mg), hindgut (Hg), gill (Gi), red muscle (Rm) and white muscle (Wm). β actin served as an internal control to calibrate the cDNA template for all of the samples.

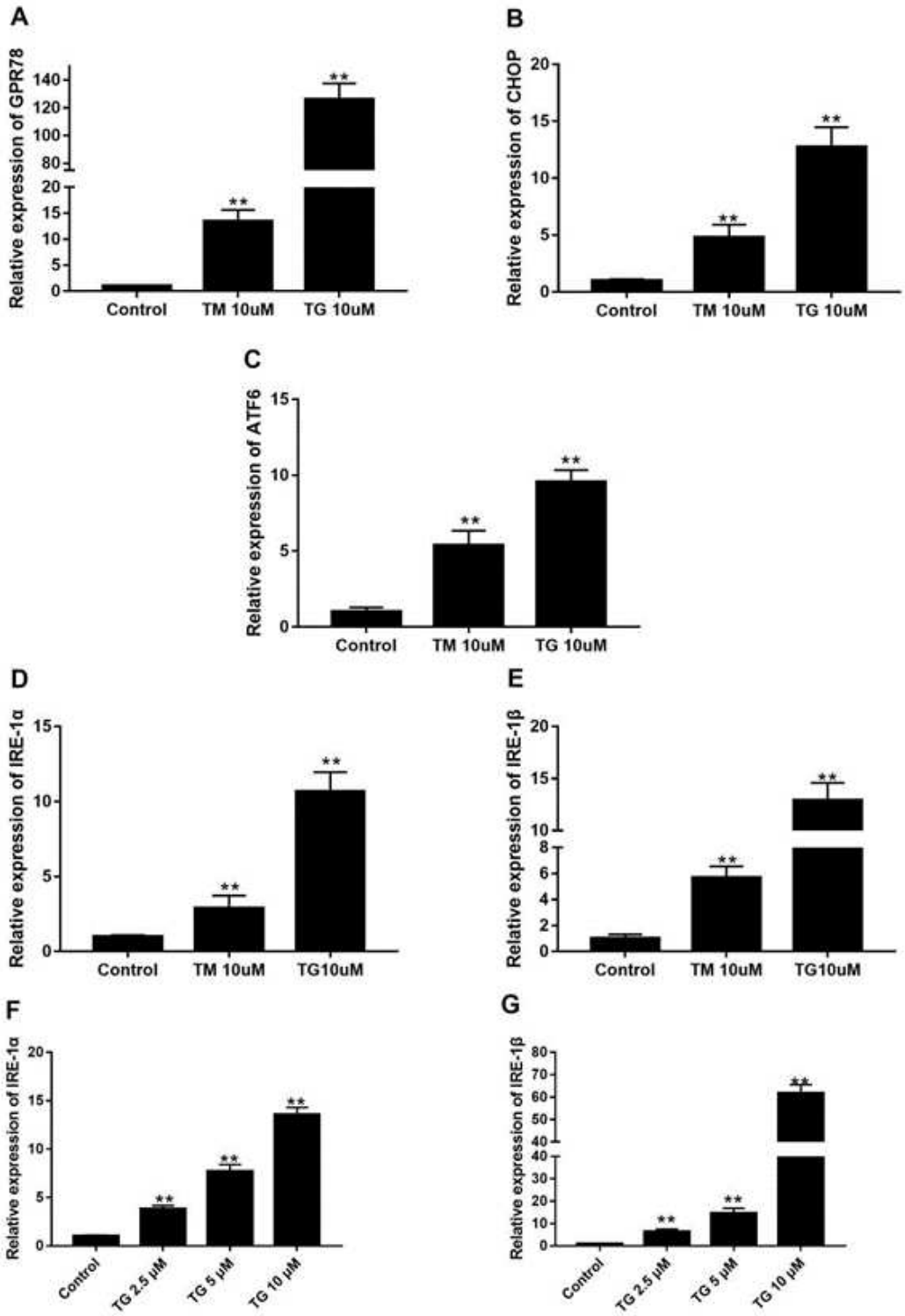

Figure 4

IRE1α and IRE1β levels were upregulated in response to ER stress in CIK cells. Cells were treated with TM 10 μM) and TG (0, 2. 5, 5 , or 1 0 μM) for 24 hours . The relative mRNA levels were detected by R eal time PCR

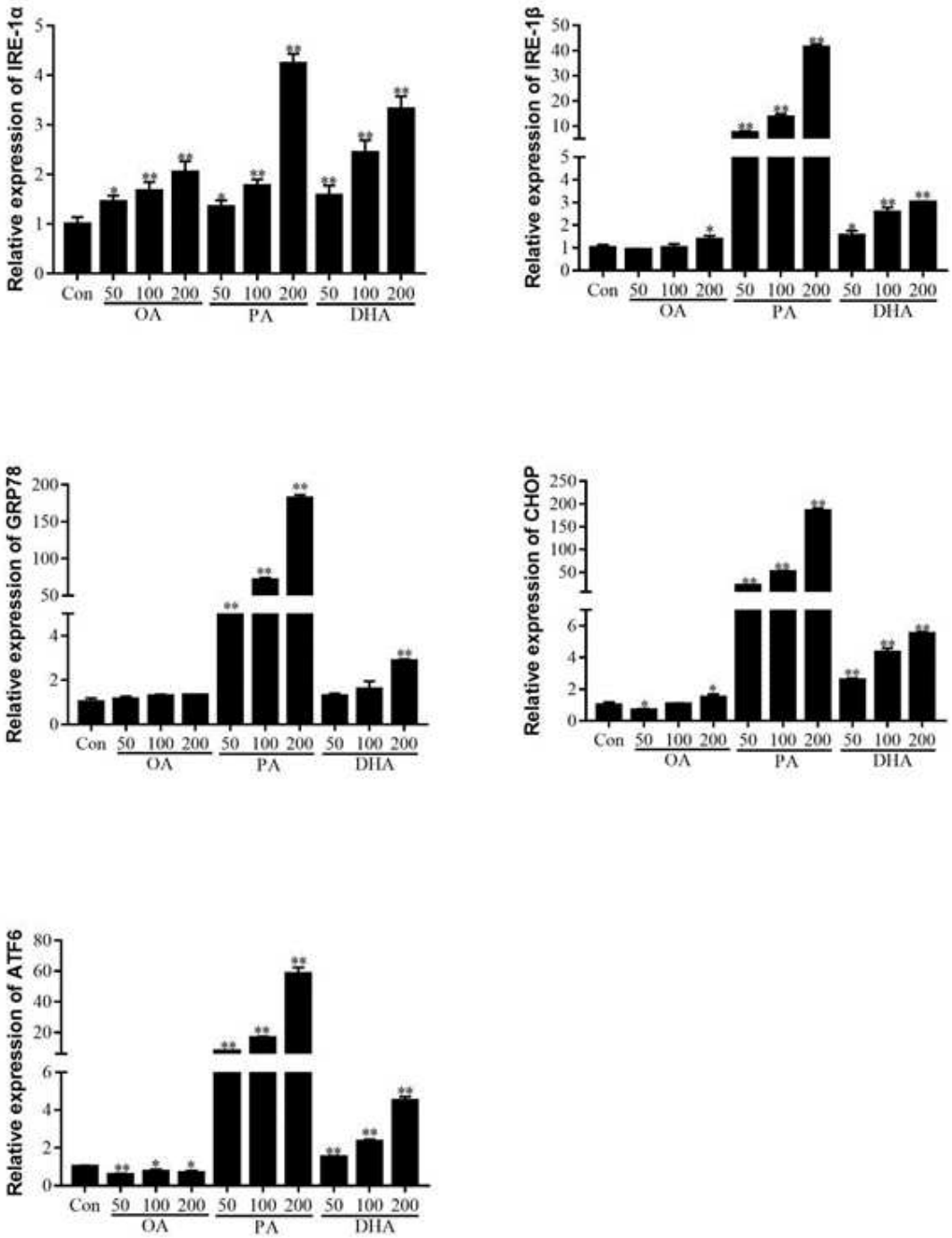

Figure 5

Effects of fatty acids on ER stress in CIK cells CIK cells were incubated with various concentrations of fatty acids for 24 hours C ells treated with BSA as the control, after incubation, Total RNA was extracted and then quantified using Real time PCR.

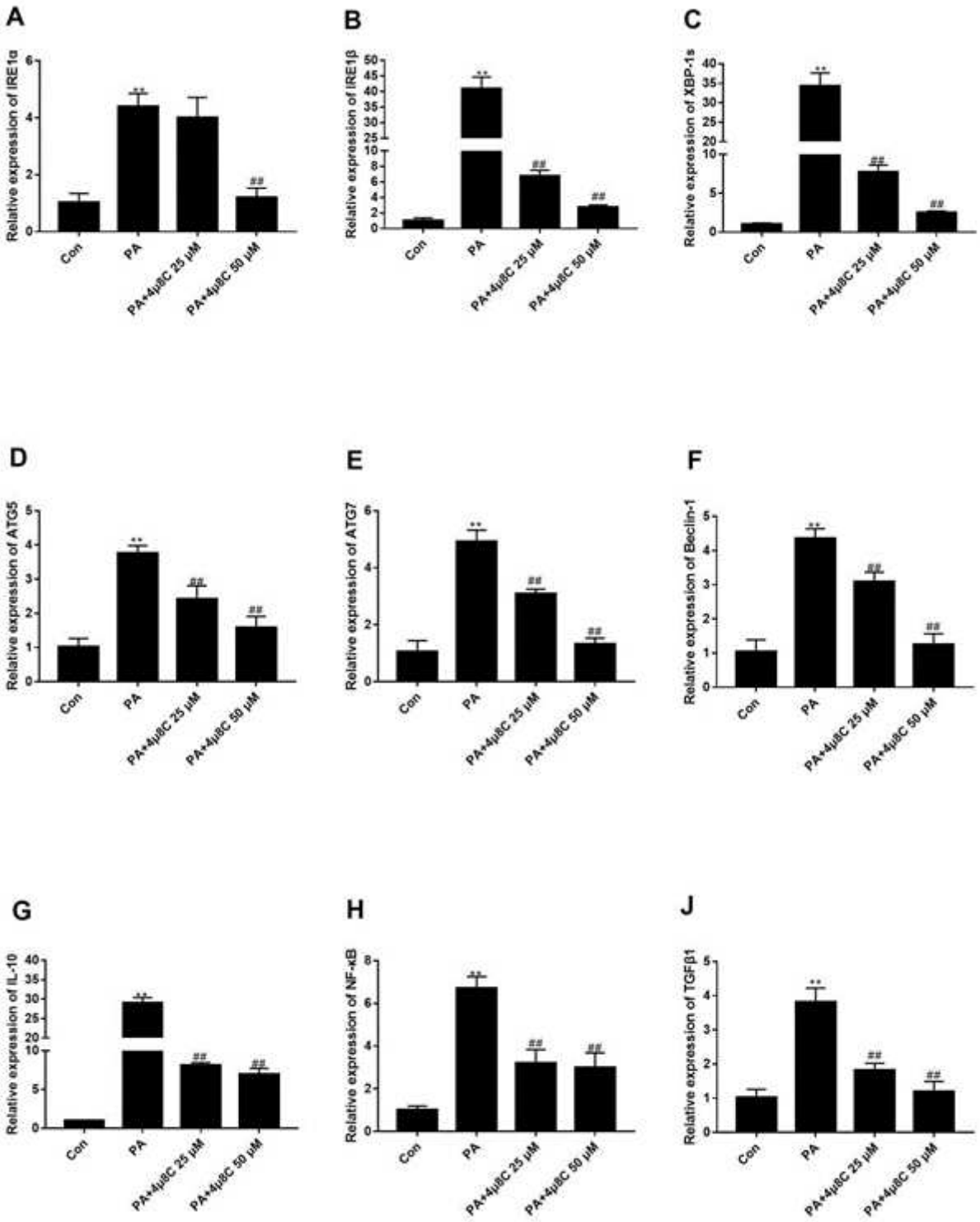

Figure 6

Inhibition of IRE1α ameliorates PA induced autophagy and inflammation CIK cells were later either pretreated with 4μ8C for 4 h, followed by treatment with PA (200 μM) for 24 h. CIK cells treated with vehicle (DMSO) and BSA were used for control. Total RNA was extracted and then quantified using Real time PCR. *significantly different compared with controls (P < 0.05); # 401 significantly different compared with PA (P 0.05).

Supplementary Files

This is a list of supplementary files associated with this preprint. Click to download.

- Supplement.pdf